J. Biochem. 2009;146(4)571–579
doi:10.1093/jb/mvp101

Identification of Radicals Formed in the Reaction Mixture of Bovine Kidney Microsomes with NADPH

Kazumasa Kumamoto[1,2], Tomihiro Hirai[3], Shiroh Kishioka[1] and Hideo Iwahashi[2,*]

[1]Department of Pharmacology; [2]Department of Chemistry, Wakayama Medical University, 811-1 Kimiidera, Wakayama 641-8509; and [3]Department of Sport and Health Science, Osaka Sangyo University, 3-1-1 Nakagaito, Daito, Osaka 574-8530, Japan

Received May 24, 2009; accepted June 22, 2009; published online June 29, 2009

In order to explore the mechanism of myoglobinuric renal toxicity, detection and identification of free radicals was performed for the reaction mixtures of bovine kidney microsomes. EPR measurements showed prominent signals for the control reaction mixture containing 2.0 mg protein/ml bovine kidney microsomes, 5 mM NADPH, 0.1 M 4-POBN and 29 mM phosphate buffer (pH 7.4). Addition of myoglobin (Mb) to the control reaction mixture resulted in increase of EPR peak height. The result indicates that Mb enhances the radical formation. An HPLC–EPR measurement showed three peaks with retention times of 29.4 min (P_1), 32.4 min (P_2) and 46.6 min (P_3). HPLC–EPR–MS analyses of P_1 and P_2 gave ions at *m/z* 282. The results show that 4-POBN/hydroxypentyl radical adducts form in the reaction mixture. An HPLC–EPR–MS analysis of P_3 gave ions at *m/z* 266, indicating that 4-POBN/pentyl radical adduct forms in the reaction mixture.

Key words: electron spin resonance, kidney, lipid peroxidation, microsomes, myoglobin.

Abbreviations: EPR, electron paramagnetic resonance; 4-POBN, α-(4-pyridyl-1-oxide)-*N*-*tert*-butylnitrone; HPLC, high performance liquid chromatography; MS, mass spectrometry; Mb, myoglobin; ROS, reactive oxygen species; NTA, nitrilotriacetic acid; EDTA, ethylenediaminetetraacetic acid; DTPA, diethylenetriaminepentaacetic acid; DFO, deferoxamine; 13-HPODE, 13-hydroperoxy-9,11-octadecadienoic acid.

It is well known that excessive muscle activity or overexertion, such as excessive bodybuilding, may cause rhabdomyolysis, the release of myoglobin (Mb) from skeletal muscle (*1*). Rhabdomyolysis has been implicated as a significant cause of acute renal failure and may be attributable for up to 7–10% of cases of acute renal failure.

Several experimental models have been used to explore the mechanism of myoglobinuric renal toxicity (*2–4*). There is now considerable evidence that lipid peroxidation occurs in rhabdomyolysis (*5*, *6*). The current literature supports the hypothesis of free radical involvement in Mb-induced renal toxicity. Mb, heme and free iron ion have all been suggested as the chemical forms responsible for renal toxicity (*7–9*). There are multiple sources of reactive oxygen species (ROS), including mitochondrial electron transport, cyclooxygenases, lipoxygenases, and mixed-function oxidases of the endoplasmic reticulum, xanthine oxidase system and tubule cell plasma membrane NADPH oxidase (*10*, *11*). We have focused on the effects of Mb on the ROS generation in mixed-function oxidases of the endoplasmic reticulum in this article (*12*), because the proximal tubule is especially rich in cytochrome P450 and the principal target of celluar damage in myoglobinuric acute renal failure.

In spite of the intensive EPR studies, many radical species have not been identified. In this study, identification of the free radicals has been performed for the reaction mixture containing bovine kidney microsomes, NADPH, ADP, $FeCl_3$ and phosphate buffer (pH 7.4) using high performance liquid chromatography–electron paramagnetic resonance spectrometry (HPLC–EPR) and high performance liquid chromatography–electron paramagnetic resonance–mass spectrometry (HPLC–EPR–MS) (*13*).

MATERIALS AND METHODS

Materials—α-(4-Pyridyl-1-oxide)-*N*-*tert*-butylnitrone (4-POBN: spin-trapping reagent) and nitrilotriacetic acid disodium salt (NTA) were purchased from Tokyo Kasei Kogyo, Ltd. (Tokyo, Japan). Ferrous ammonium sulfate and 1-pentanol were obtained from Kishida Chem. Co. (Osaka, Japan). Ethylenediaminetetraacetic acid disodium salt (EDTA), ferric chloride, ADP and NADPH were from Wako Pure Chemical Industries, Ltd. (Osaka, Japan). Diethylenetriaminepentaacetic acid (DTPA) was obtained from Nakarai Chemicals Ltd. (Kyoto, Japan). Horse skeletal muscle Mb and deferoxamine mesylate salt (DFO) were purchased from Sigma-Aldrich Co. (St Louis, MO, USA). Sep-pak C_{18} was from Waters Associates (Milford, MA, USA). Pentylhydrazine oxalate was synthesized according to the method of Gever and Hayes (*14*). Water used in these experiments was purified by passing through Milli-Q Jr (Nihon Millipore Kogyo K.K., Yonezawa, Japan) after distillation. All other chemicals used were of analytical grade.

*To whom correspondence should be addressed. Tel/Fax: +81-73-441-0772, E-mail: chem1@wakayama-med.ac.jp

Preparation of 13-Hydroperoxy-9,11-Octadecadienoic acid (13-HPODE)—Preparation of 13-HPODE was performed as described in the previous paper (*15*).

Preparation of Bovine Kidney Microsomes—A bovine kidney microsomes were used in the experiments. The bovine kidney was removed immediately after a bovine was sacrificed and followed by exsanguination. The kidney was homogenized in 9 volumes of 0.25 M sucrose. The kidney homogenate was centrifuged at 16 000 g for 30 min at 4°C. The supernatant fraction was then centrifuged at 120 000 g for 30 min at 4°C. The pallet was suspended in 0.15 M KCl and then centrifuged twice again at 120 000 g. The pallet was suspended in 0.15 M KCl. Protein concentration of the suspension was 15.7 mg/ml. It was kept at −80°C before use.

Preparation of 4-POBN/Pentyl Radical Adduct—4-POBN/pentyl radical adduct was synthesized through the decomposition of pentylhydrazine (*16*). The reaction mixture contained 0.1 M 4-POBN, 2.5 mg/ml pentylhydrazine oxalate, 0.2 mM $CuCl_2$ and 44 mM carbonate buffer (pH 10.0). After nitrogen gas was bubbled through the reaction mixture without $CuCl_2$ for 5 min, the reaction was started by adding $CuCl_2$. The reaction was performed for 2 h at 25°C.

Reaction of 1-Pentanol with Fenton Reaction System—4-POBN/hydroxypentyl radical adducts were synthesized through the reaction of 1-pentanol with Fenton reaction system. The reaction mixture of 1-pentanol with Fenton reaction system contained 0.1 M 4-POBN, 0.5% (v/v) 1-pentanol, 0.1 mM H_2O_2, 0.1 mM $FeSO_4(NH_4)_2SO_4$ and 39 mM phosphate buffer (pH 7.4). The reaction was started by adding $FeSO_4(NH_4)_2SO_4$. The reaction was performed for 2 min at 25°C.

The Control Reaction Mixture—The control reaction mixture contained 2.0 mg protein/ml bovine kidney microsomes, 5 mM NADPH, 0.1 M 4-POBN and 29 mM phosphate buffer (pH 7.4). The reaction was started by adding NADPH. The reaction was performed for 60 min at 37°C.

Complete Reaction Mixture of 13-HPODE with Mb—The complete reaction mixture of 13-HPODE with Mb contained 0.14 mM 13-HPODE, 5 mM NADPH, 5 μM Mb, 0.1 M 4-POBN and 40 mM phosphate buffer (pH 7.4). The reaction was started by adding 13-HPODE. The reaction was performed for 2 min at 25°C.

Complete Reaction Mixture of 13-HPODE with $FeCl_3$—The complete reaction mixture of 13-HPODE with $FeCl_3$ contained 0.14 mM 13-HPODE, 5 mM NADPH, 10 μM $FeCl_3$, 0.1 M 4-POBN and 25 mM phosphate buffer (pH 7.4). The reaction was started by adding 13-HPODE. The reaction was performed for 2 min at 25°C.

Visible Absorption Spectroscopy—The visible absorption spectra of the samples were taken using UV-160A UV–Visible Recording Spectrophotometer (Shimadzu, Ltd, Kyoto, Japan). The sample contained 96.7 μM Mb (or 96.7 μM Mb with 96.7 μM EDTA) in 50 mM phosphate buffer (pH 7.4).

EPR Measurements—The EPR spectra were obtained using a model JES-FR30 Free Radical Monitor (JEOL Ltd, Tokyo, Japan). Aqueous samples were aspirated into a Teflon tube centered in a microwave cavity. Operating conditions of the EPR spectrometer were: power, 4 mW; modulation width, 0.1 mT; center of magnetic field, 337.000 mT; sweep time, 4 min; sweep width, 10 mT; and time constant, 0.3 s. Magnetic fields were calculated by the splitting of MnO ($\Delta H3$–4 = 8.69 mT).

HPLC–EPR Chromatography—An HPLC used in the HPLC–EPR consisted of a model 7125 injector (Reodyne, Cotati, CA, USA), a model 655A-11 pump with a model L-5000 LC controller (Hitachi Ltd, Ibaragi, Japan). A semi-preparative column (300 mm long × 10 mm i.d.) packed with TSKgel ODS-120T (Tosoh Co., Tokyo, Japan) was used. Flow rate was 2.0 ml/min throughout the HPLC–EPR experiments. For the HPLC–EPR, two solvents were used: solvent A, 50 mM ammonium acetate; and solvent B, 50 mM ammonium acetate/acetonitrile (36 : 64, v/v). A following combination of isocratic and linear gradient was used: 0–40 min, 100% A to 0% A (linear gradient); 40–60 min, 100% B (isocratic). The eluent was introduced into a model JES-FR30 Free Radical Monitor (JEOL Ltd, Tokyo, Japan). The EPR spectrometer was connected to the HPLC with a Teflon tube, which passed through the center of the EPR cavity. The operating conditions of the EPR spectrometer were: power, 4 mW; modulation width, 0.2 mT; and time constant, 1 s. The magnetic field was fixed at the third peak in the doublet–triplet EPR spectrum ($\alpha^N = 1.58$ mT and $\alpha^H\beta = 0.26$ mT) of the 4-POBN radical adduct (Fig. 1).

HPLC–EPR–MS Chromatography—HPLC and EPR conditions were as described in the HPLC–EPR. The operating conditions of the mass spectrometer were: nebulizer, 180°C; aperture 1, 120°C; N_2 controller pressure, 19.6 N/cm^2; drift voltage, 70 V; multiplier voltage

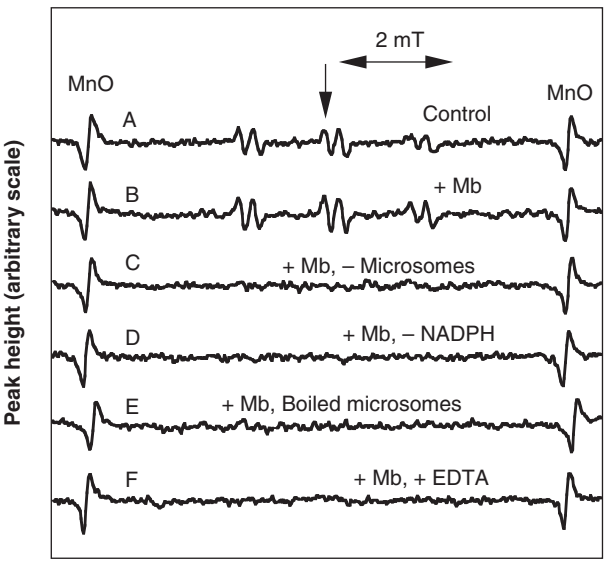

Fig. 1. **EPR spectra of the control reaction mixtures.** The reaction and EPR conditions were as described under MATERIALS AND METHODS section. (A) Control reaction mixture. (B) Same as in (A) except that 5 μM Mb was added. (C) Same as in (B) except that bovine kidney microsomes were omitted. (D) Same as in (B) except that NADPH was omitted. (E) Same as in (B) except that bovine kidney microsomes were boiled for 3 min and used for the reaction. (F) Same as in (B) except that 0.1 mM EDTA was added.

1800 V; needle voltage, 3000 V; polarity, positive; and resolution, 48.

The mass spectra were obtained by introducing the eluent from the EPR detector into the LC–MS system just before the respective peaks were eluted. The flow rate was kept at 50 μl/min while the eluent was introduced into the mass spectrometer.

RESULTS

EPR Measurements of the Control Reaction Mixture—EPR spectra of the control reaction mixtures were measured (Fig. 1). A prominent EPR spectrum ($\alpha^N = 1.58$ mT and $\alpha^H\beta = 0.26$ mT) was observed for the control reaction mixture (Fig. 1A). On addition of Mb to the control reaction mixture, the EPR peak height increased to 133 ± 9% of the control reaction mixture (Fig. 1B). In the absence of bovine kidney microsomes (or NADPH), the EPR spectrum was hardly observed for the control reaction mixture with Mb (Fig. 1C and D). For the control reaction mixture of boiled microsomes with Mb, the EPR signals disappeared (Fig. 1E). On addition of EDTA to the control reaction mixture with Mb, the EPR signals were scarcely observed (Fig. 1F).

Effects of Several Iron Chelators on the Reaction—In order to know whether EDTA interacts with the iron ion in Mb, visible spectrum of Mb (or Mb with EDTA) was measured (Fig. 2). The two visible spectra were quite identical. The results indicate that EDTA does not interact with the iron ion in Mb.

The effects of several iron chelators (EDTA, NTA, DTPA and DFO) on the reaction were examined (Fig. 3). On addition of EDTA (or DTPA, or DFO) to the control reaction mixture, the EPR signals were hardly observed. On the other hand, addition of NTA resulted in the increment of EPR peak height (135 ± 2% of control reaction mixture).

Effects of ADP and its derivatives on the reaction were examined for the control reaction mixture with $FeCl_3$ (Fig. 4). Addition of adenosine (or AMP) showed

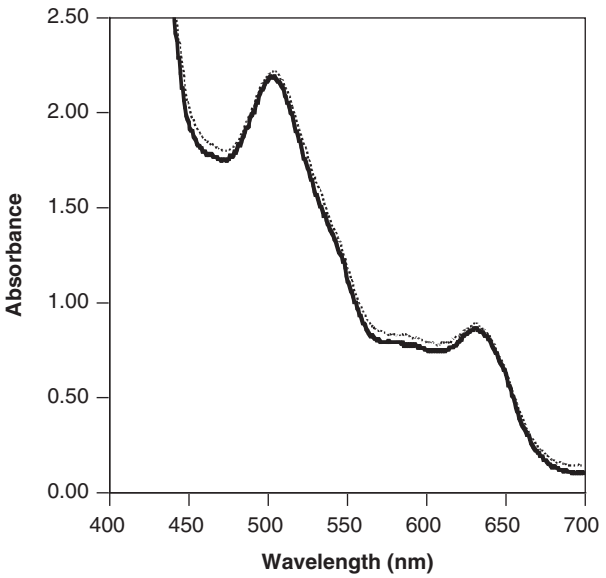

Fig. 2. **Visible absorption spectrum of Mb (or Mb with EDTA).** Conditions of the samples and measurements were as described under MATERIALS AND METHODS section. Dotted lines, 96.7 μM Mb in 50 mM phosphate buffer (pH 7.4); and solid line, 96.7 μM Mb with 96.7 μM EDTA in 50 mM phosphate buffer (pH 7.4).

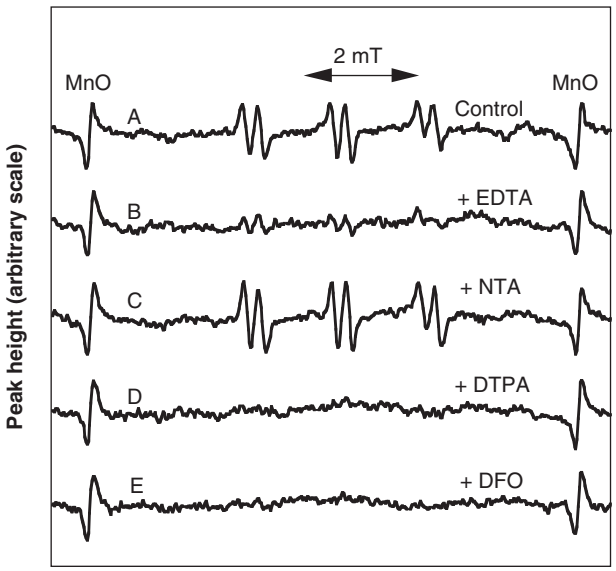

Fig. 3. **EPR analyses of the control reaction mixtures with several iron chelators.** The reaction and EPR conditions were as described under MATERIALS AND METHODS section. (A) Control reaction mixture. (B) Same as in (A) except that 0.1 mM EDTA was added. (C) Same as in (A) except that 0.1 mM NTA was added. (D) Same as in (A) except that 0.1 mM DTPA was added. (E) Same as in (A) except that 0.1 mM DFO was added.

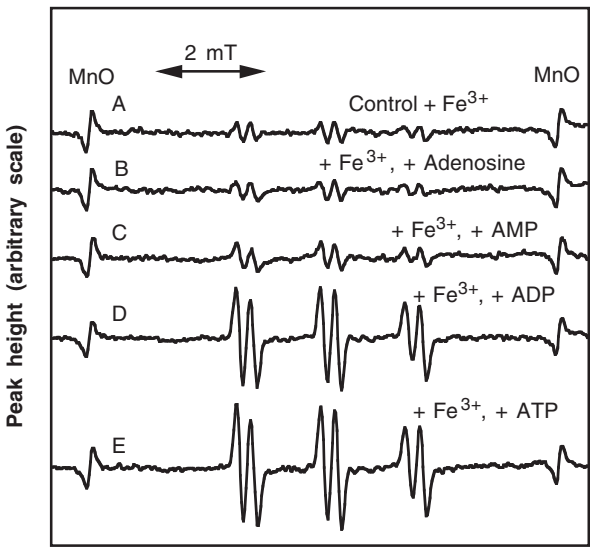

Fig. 4. **Effects of ADP derivatives on the radical formation in the control reaction mixtures with $FeCl_3$.** The reaction and EPR conditions were as described under MATERIALS AND METHODS section. (A) Control reaction mixture with 0.17 mM $FeCl_3$. (B) Same as in (A) except that 10 mM adenosine was added. (C) Same as in (A) except that 10 mM AMP was added. (D) Same as in (A) except that 10 mM ADP was added. (E) Same as in (A) except that 10 mM ATP was added.

no effect (adenosine, 89 ± 6% of control reaction mixture with Fe^{3+}; and AMP, 110 ± 17% of control reaction mixture with $FeCl_3$). On addition of ADP (or ATP), the EPR peak height increased to 562 ± 63% of control reaction mixture with $FeCl_3$ (or 533 ± 34% of control reaction mixture with $FeCl_3$). On the other hand, addition of ADP to the control reaction mixture resulted in a little increase of EPR peak height (126 ± 12% of the control) (data not shown). These results indicate that a complex of ADP (or ATP) with iron ion accelerates the radical formation.

Effects of Several Metal Ions on the Reaction—The effects of several metal ions such as Fe^{2+}, Fe^{3+}, Ca^{2+}, Mg^{2+}, Cu^{2+} and Zn^{2+} on the reaction were examined (Fig. 5, Table 1). On addition of Fe^{2+} to the control reaction mixture, the EPR peak height slightly increased. Addition of Fe^{3+} (or Ca^{2+} or Mg^{2+}) to the control reaction mixture showed no effect on the EPR peak height. Addition of Cu^{2+} (or Zn^{2+}) resulted in decrease of the EPR peak height.

EPR Analyses of the Complete Reaction Mixture of 13-HPODE with Mb—To clarify whether Mb catalyzes the radical formation in the reaction mixture containing hydroperoxides, EPR analysis was performed for the complete reaction mixture containing 13-HPODE and Mb (Fig. 6). This analysis showed prominent signals (Fig. 6A). On the other hand, the EPR signal was hardly observed for the complete reaction mixture without Mb (Fig. 6B). The result indicates that Mb catalyzes the radical formation in the complete reaction mixture of 13-HPODE with Mb. No EPR signal was observed for the complete reaction mixture without 13-HPODE (Fig. 6D), suggesting that the radicals are derived from 13-HPODE. On addition of EDTA, the EPR peak height remained unchanged (107 ± 6% of the complete reaction mixture) (Fig. 6C).

EPR Analyses of the Complete Reaction Mixture of 13-HPODE with $FeCl_3$—To know whether $FeCl_3$ catalyzes the radical formation in the reaction mixture containing hydroperoxides, EPR analysis was performed for the complete reaction mixture of 13-HPODE with $FeCl_3$ (data not shown). The complete reaction mixture of 13-HPODE with $FeCl_3$ contained 0.14 mM 13-HPODE, 5 mM NADPH, 10 μM $FeCl_3$, 0.1 M 4-POBN and 25 mM phosphate buffer (pH 7.4). EPR analysis of the complete reaction mixture showed prominent signals (data not shown). On the other hand, a small EPR signal was observed for the complete reaction mixture without

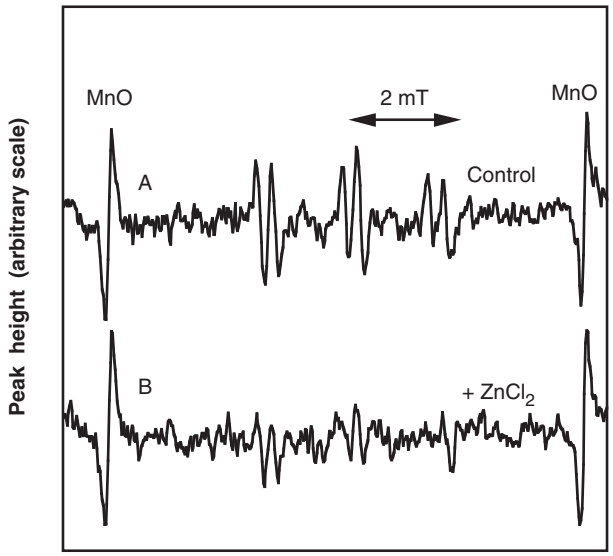

Fig. 5. **Effect of $ZnCl_2$ on the radical formation in the control reaction mixture.** The EPR and reaction conditions were as described in the MATERIALS AND METHODS section. (A) Control reaction mixture. (B) Same as in (A) except that 0.1 mM $ZnCl_2$ was added.

Table 1. **Effects of several metal ions on EPR peak height in the control reaction mixtures.**

Metal ions added (100 μM)	Relative EPR peak height (%) ± SD
Control	100
$FeSO_4(NH_4)_2SO_4$	121 ± 11
$FeCl_3$	87 ± 17
$CaCl_2$	95 ± 10
$MgCl_2$	90 ± 28
$CuCl_2$	48 ± 10
$ZnCl_2$	47 ± 13

The reaction and EPR conditions were as described under MATERIALS AND METHODS section. EPR measurements were performed for the control reaction mixture with $FeSO_4(NH_4)_2SO_4$ (or $FeCl_3$, or $CaCl_2$, or $MgCl_2$, or $CuCl_2$ or $ZnCl_2$) (0.1 mM). The data presented are mean ± SD of three independent experiments.

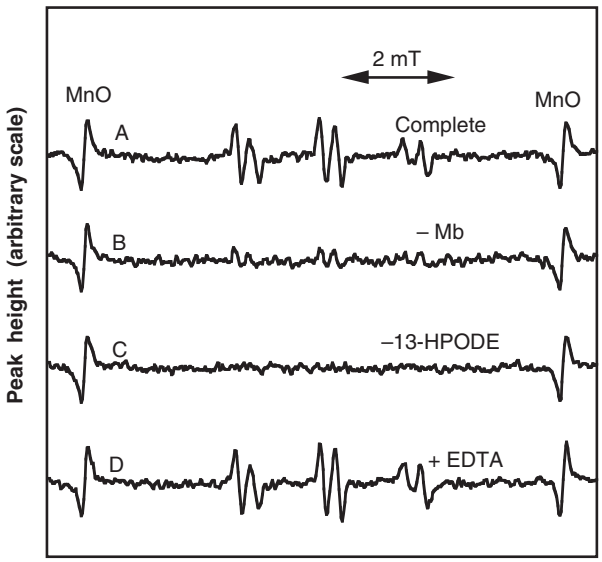

Fig. 6. **EPR analyses of the complete reaction mixtures of 13-HPODE with Mb.** The EPR conditions were as described under MATERIALS AND METHODS section. The complete reaction mixture contained 0.14 mM 13-HPODE, 5 μM Mb, 0.1 M 4-POBN and 40 mM phosphate buffer (pH 7.4). The reaction was started by adding 13-HPODE. The reaction was performed for 2 min at 25°C. (A) Complete reaction mixture of 13-HPODE with Mb. (B) Same as in (A) except that Mb was omitted. (C) Same as in (A) except that 13-HPODE was omitted. (D) Same as in (A) except that 0.1 mM EDTA was added.

13-HPODE (26 ± 13% of the complete reaction mixture), suggesting that the radicals are predominantly derived from 13-HPODE. The EPR peak height decreased for the complete reaction mixture without $FeCl_3$ (64 ± 14% of the complete reaction mixture). The result indicates that $FeCl_3$ catalyzes the radical formation in the complete reaction mixture of 13-HPODE with $FeCl_3$. The EPR peak height did not changed for the complete reaction mixture without NADPH (85 ± 16% of the complete reaction mixture). On addition of EDTA, the EPR peak height remained unchanged (100 ± 28% of the complete reaction mixture). Above results showed that neither NADPH nor EDTA affects the radical formation in the complete reaction mixture of 13-HPODE with $FeCl_3$.

HPLC–EPR and HPLC–EPR–MS Analyses of the Control Reaction Mixture with ADP and $FeCl_3$—To identify the radicals formed in the control reaction mixture with ADP and $FeCl_3$, HPLC–EPR analyses were performed. Three prominent peaks (P_1, P_2 and P_3) were separated on the HPLC–EPR elution profile of the control reaction mixture with ADP and $FeCl_3$ (Fig. 7). The retention times of the three peaks were as follows: P_1, 29.4 min; P_2, 32.4 min; P_3, 46.6 min.

To determine the chemical structure of P_1, an HPLC–EPR–MS analysis was performed for P_1. The HPLC–EPR–MS analysis of P_1 gave ions at m/z 282 (Fig. 8A). The ions at m/z 282 correspond to the protonated molecules of 4-POBN/hydroxypentyl radical adduct, $[M + H]^+$. HPLC–EPR–MS analysis of P_2 also gave ions at m/z 282 (Fig. 8B). It may be a diastereoisomer of 4-POBN/hydroxypentyl radical adducts. An HPLC–EPR–MS

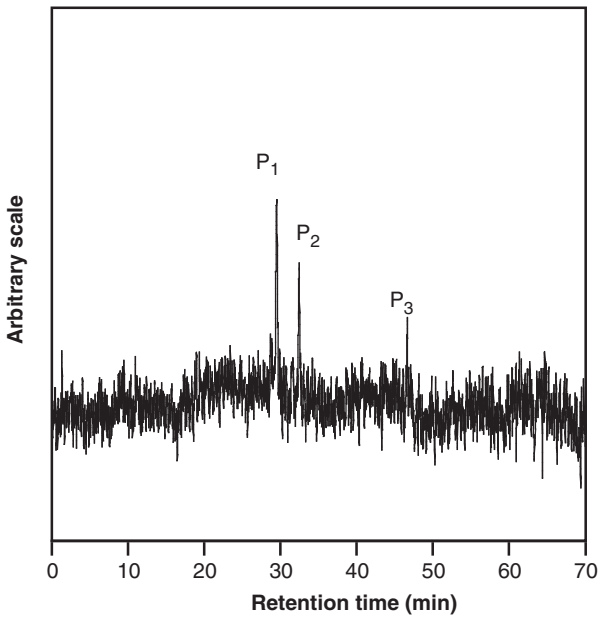

Fig. 7. **HPLC–EPR analysis of the control reaction mixtures with ADP and $FeCl_3$.** The HPLC–EPR conditions were as described under MATERIALS AND METHODS section. The reaction mixture contained 2.0 mg protein/ml bovine kidney microsomes, 5 mM NADPH, 10 mM ADP, 0.17 mM $FeCl_3$, 0.1 M 4-POBN and 29 mM phosphate buffer (pH 7.4) in the total volume of 3.85 ml. The reaction was performed for 60 min at 37°C.

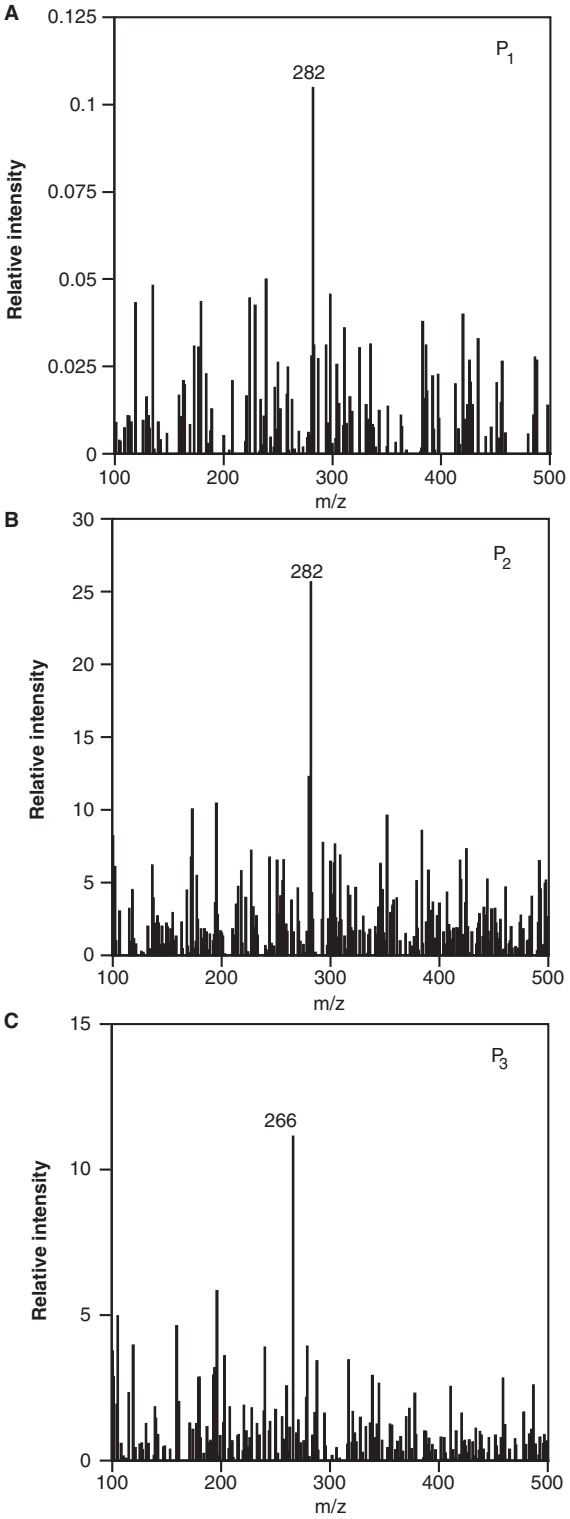

Fig. 8. **HPLC–EPR–MS analyses of the control reaction mixtures with ADP and $FeCl_3$.** The HPLC–EPR–MS conditions were as described under MATERIALS AND METHODS section. The reaction mixture contained 2.0 mg protein/ml bovine kidney microsomes, 5 mM NADPH, 10 mM ADP, 0.17 mM $FeCl_3$, 0.1 M 4-POBN and 29 mM phosphate buffer (pH 7.4) in the total volume of 11.5 ml. The reaction was performed for 60 min at 37°C. (A) A mass spectrum of P_1. (B) A mass spectrum of P_2. (C) A mass spectrum of P_3.

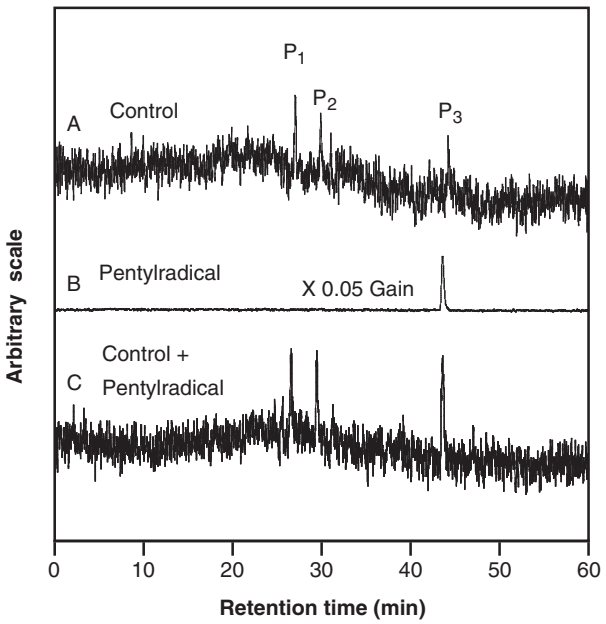

Fig. 9. **Identification of P_3.** The reaction and HPLC–EPR conditions were as described in MATERIALS AND METHODS section. (A) An HPLC–EPR analysis of the control reaction mixture with 0.17 mM $FeCl_3$ and 10 mM ADP (3.85 ml). (B) An HPLC–EPR analysis of the 4-POBN/pentyl radical adduct (10 μl). (C) The 4-POBN/pentyl radical adduct (1 μl) was added to the control reaction mixture with 0.17 mM $FeCl_3$ and 10 mM ADP (3.85 ml). An HPLC–EPR analysis of the mixture was performed.

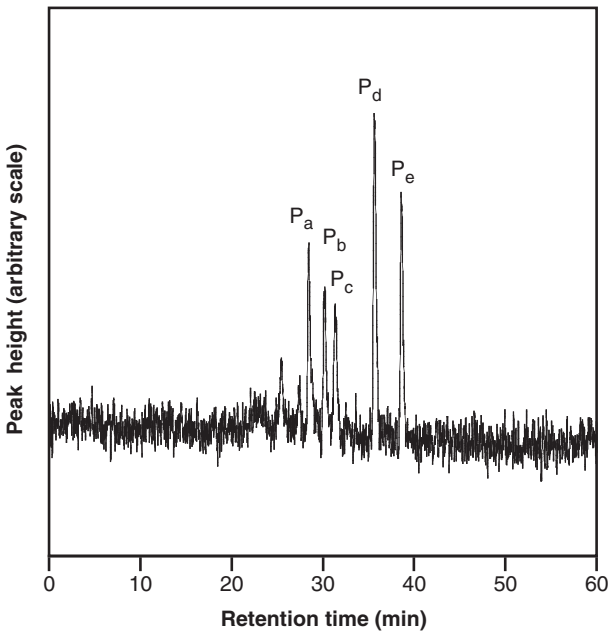

Fig. 10. **An HPLC–EPR analysis of the reaction mixture of 1-pentanol with Fenton reaction system.** The reaction and HPLC–EPR conditions were as described in MATERIALS AND METHODS section. Total volume of the reaction mixture of 1-pentanol with Fenton reaction system was 5.0 ml.

analysis of P_3 gave ions at m/z 266 (Fig. 8C). The ions at m/z 266 correspond to the protonated molecules of 4-POBN/pentyl radical adduct, $[M+H]^+$.

In order to confirm the chemical structure of P_3, HPLC–EPR analyses were performed for the reaction mixture of pentylhydrazine with Cu^{2+}. It is well known that pentyl radical forms in the reaction mixture of pentylhydrazine with Cu^{2+} (*16*). An HPLC–EPR analysis of the reaction mixture of pentylhydrazine with Cu^{2+} gave a peak with almost the same retention time as P_3 (Fig. 9B). When the peak fraction in the reaction mixture of pentylhydrazine with Cu^{2+} was mixed with the control reaction mixture with ADP and $FeCl_3$, the peak height of P_3 increased (Fig. 9C), suggesting that P_3 and 4-POBN/pentyl radical adduct are identical.

To confirm the chemical structure of P_1 and P_2, an HPLC–EPR analysis of the reaction mixture of 1-pentanol with Fenton reaction system was performed. Five prominent peaks (P_a, P_b, P_c, P_d and P_e) were observed on the HPLC–EPR elution profile of the reaction mixture of 1-pentanol with Fenton reaction system at the retention times of 28.5, 30.2, 31.4, 35.6 and 38.6 min, respectively (Fig. 10). HPLC–EPR–MS analyses showed ions at 282 m/z for all the five peaks. The results indicate that the five peaks are isomers of 4-POBN/hydroxypentyl radical adducts. Based on the retention times of the HPLC–EPR, P_a and P_c seem to be identical to P_1 and P_2, respectively. Furthermore, when the peak fraction of P_a (or P_c) was mixed with the control reaction mixture with ADP and $FeCl_3$, the peak height of P_1 (or P_2) increased (Fig. 11), indicating that P_1 (or P_2) is an isomer of hydroxypentyl radicals.

DISCUSSION

In this study, the control reaction mixture of bovine kidney microsomes with NADPH was analyzed using EPR in combination with spin trapping technique (Fig. 1). A prominent EPR spectrum ($\alpha^N = 1.58$ mT and $\alpha^H\beta = 0.26$ mT) was observed in the control reaction mixture. The EPR spectrum was hardly observed for the control reaction mixture without bovine kidney microsomes. The radicals could be derived from microsomal components. For the control reaction mixture with boiled microsomes, the EPR signals disappeared, suggesting that enzymes such as cytochrome P450 participate in the reaction.

On addition of an iron ion chelator EDTA (or DTPA, or DFO), the EPR signals disappeared (Fig. 3). On the other hand, addition of NTA (or ADP, or ATP) resulted in the increase of EPR peak height (Figs 3 and 4). These results indicate that chelator–iron ion complexes seem to play an important role in this reaction. Chelatate compounds seem to affect the radical formation to a great extent. Addition of Zn^{2+} (or Cu^{2+}) resulted in decrease of EPR peak height (Fig. 5, Table 1). The displacement of iron ion by Zn^{2+} (or Cu^{2+}) in the active chelator–iron ion complexes may cause the inhibitory effects. In addition to the above possible mechanism, Cu^{2+} may inhibit the radical formation by changing the redox state of the reaction. In the case of Ca^{2+} and Mg^{2+}, no effect was observed

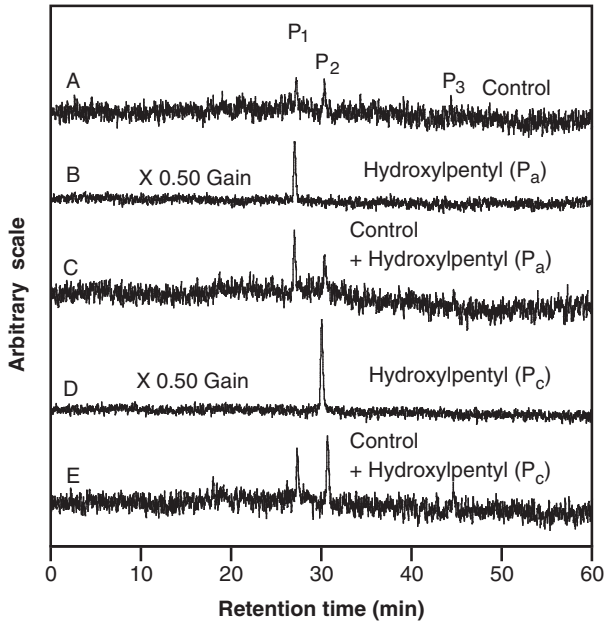

Fig. 11. **Identification of P_1 and P_2.** The reaction and HPLC-EPR conditions were as described in MATERIALS AND METHODS section. (A) An HPLC–EPR analysis of the control reaction mixture with 0.17 mM $FeCl_3$ and 10 mM ADP (3.85 ml). (B) An HPLC–EPR analysis of P_a in reaction mixture of 1-pentanol with Fenton reaction system (160 μl). (C) P_a (55 μl) was added to the control reaction mixture with 0.17 mM $FeCl_3$ and 10 mM ADP (3.85 ml). An HPLC–EPR analysis of the mixture was performed. (D) An HPLC–EPR analysis of P_c in reaction mixture of 1-pentanol with Fenton reaction system (0.25 ml). (E) P_c (46 μl) was added to the control reaction mixture with 0.17 mM $FeCl_3$ and 10 mM ADP (3.85 ml). An HPLC–EPR analysis of the mixture was performed.

for the radical formation. The competitions between Ca^{2+} (or Mg^{2+}) and iron ions may not occur in this reaction. On addition of $FeSO_4(NH_4)_2SO_4$ (or $FeCl_3$), the EPR peak height hardly changed. Chelate compounds may not be enough for $FeSO_4(NH_4)_2SO_4$ (or $FeCl_3$).

Addition of Mb to the control reaction mixture resulted in increase of EPR peak height, suggesting that Mb catalyzes the radical formation at a step during the control reaction (Fig. 1B). Indeed, Mb enhanced the radical formation in the complete reaction mixture of 13-HPODE with Mb (Fig. 6). These results indicate that Mb accelerates the radical-formation step from hydroperoxides (LOOH) in the control reaction (Scheme 1). Since iron ions also enhanced the radical formation in the complete reaction mixture of 13-HPODE with Fe^{3+}, iron ions seem to catalyze the radical-formation step from hydroperoxides (Scheme 1). Addition of EDTA completely inhibited the radical formation in the control reaction mixture (Fig. 3B), but did not inhibited the one in the complete reaction mixture of 13-HPODE with Mb (or $FeCl_3$) (Fig. 6C). These results suggest that EDTA inhibits the LOOH-generation step in the control reaction (Scheme 1). On the other hand, Mb seems to catalyze the radical-formation step from the LOOH, but not the LOOH-generation step in the control reaction (Scheme 1), because EDTA did not interact with iron

Microsomes/NADPH/Fe^{3+}/Mb Reaction System

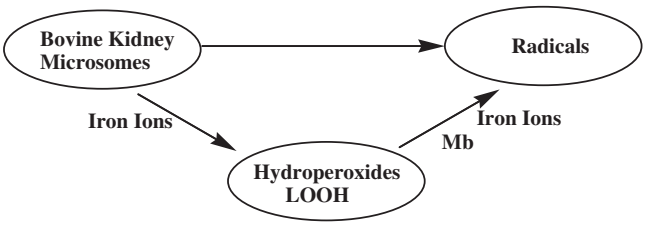

Scheme 1. **Iron ions catalyze two steps from microsomal lipid to hydroperoxides and from hydroperoxides to radicals, and Mb catalyzes the step from hydroperoxides to radicals.**

ion in Mb. EDTA may inhibit the LOOH-generation step by forming EDTA–Fe complex.

HPLC–EPR and HPLC–EPR–MS analyses showed that 4-POBN/hydroxypentyl radical and 4-POBN/pentyl radical adducts form in the control reaction mixture with ADP and Fe^{3+}. A possible reaction path for the formation of the radicals (hydroxypentyl and pentyl radicals) are shown as follows (Scheme 2). Reaction of NADPH/microsomes with unsaturated fatty acids LH such as linoleic acid and arachidonic acid results in allyl radical $L^{\bullet}$ (Scheme 2). Peroxyl radical $LOO^{\bullet}$ possibly forms through the reaction of the allyl radical $L^{\bullet}$ with molecular oxygen O_2 (Scheme 2). The peroxyl radicals $LOO^{\bullet}$ turn to hydroperoxides LOOH by removing $H^{\bullet}$ from surrounding molecules (Scheme 2). Mb [Mb-Fe(III)] catalyzed homolytic scission of the hydroperoxide LOOH (Fig. 6). Rota *et al*. reported that cytochrome P450 also catalyzes homolytic scission of hydroperoxides LOOH (*17*). This reaction yields radical intermediates $LO^{\bullet}$ (*18*) (Scheme 2). β-Scission of the $LO^{\bullet}$ possibly results in the generation of pentyl radical. Thus, oxidation of ω6 series of unsaturated fatty acids could form the pentyl radical (Scheme 2).

Reaction of the pentyl radical with molecular oxygen O_2 may form 1-hydroperoxypentane through the path described in Scheme 2. 1-Pentoxyl radical forms via a reaction of 1-hydroperoxypentane with hemoproteins such as [Mb-Fe(III)] and cytochrome P450 (or ferrous ions). 1-Methyl-4-hydroxybutyl radical may form from the 1-pentoxyl radical by 1,5-hydrogen shifts via six-membered ring transition state. Intraradical six-membered activated complex has been demonstrated on frequent isomerization of alkoxyl radicals (*19*, *20*). Indeed, isomerization of the 2-pentoxyl radical by 1,5-hydrogen shifts via a low-strain six-membered ring transition state has the activation energy 40 kJ/mol and a relatively high frequency factor of the order $10^{11}\,sec^{-1}$ (*21*). Two HPLC–EPR peaks (P_1 and P_2) were observed (Fig. 7). Because two asymmetric carbon atoms (*) exist in the 4-POBN/1-methyl-4-hydroxybutyl radical adducts (Fig. 12), P_1 and P_2 appear to be the two diastereoisomers of the 4-POBN/1-methyl-4-hydroxybutyl radical adducts.

Five prominent peaks (P_a, P_b, P_c, P_d and P_e) were observed for the reaction mixture of 1-pentanol with Fenton reaction system. Based on mass spectra data,

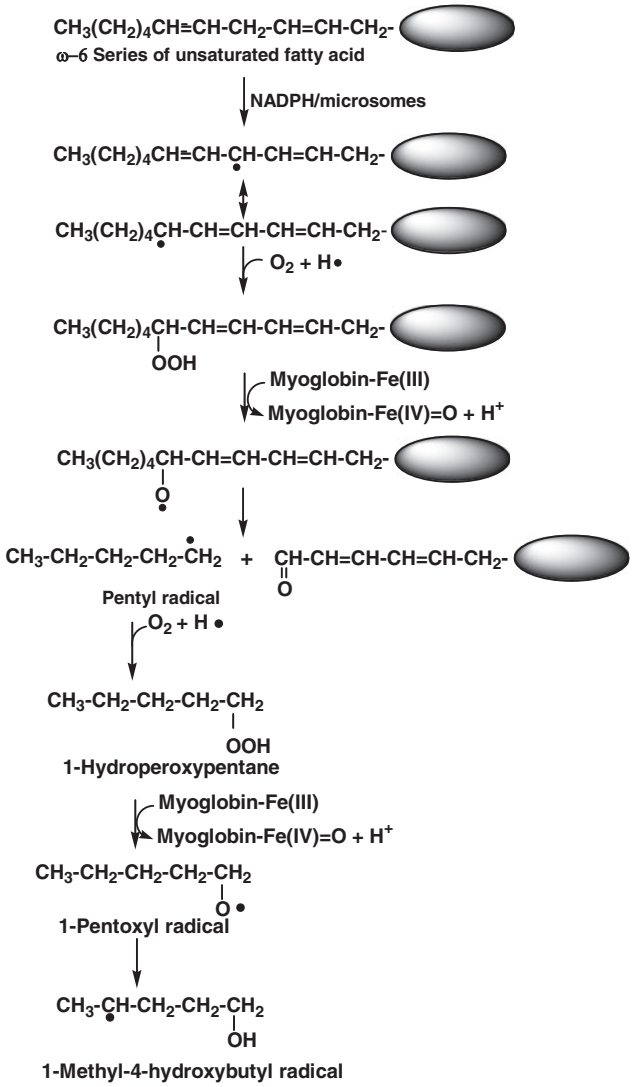

Scheme 2. **A possible path for the formation of pentyl and 1-methyl-4-hydroxybutyl radicals from ω-6 series of unsaturated fatty acid in kidney microsomes/NADPH/Fe^{3+}/Mb reaction system.**

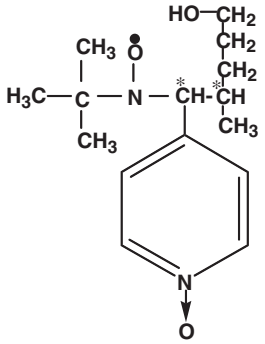

Fig. 12. **Chemical structure of 4-POBN/1-methyl-4-hydroxybutyl radical adduct.** Asymmetric carbon atoms are indicated by asterisk marks.

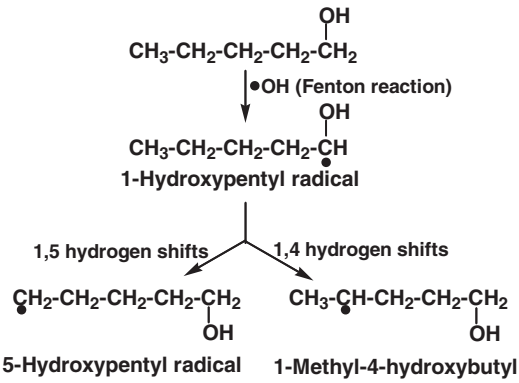

Scheme 3. **A possible path for the formation of 1-hydroxypentyl, 5-hydroxypentyl and 1-methyl-4-hydroxybutyl radicals in the reaction of 1-pentanol with Fenton reaction system.**

all of the five peaks appear to be isomers of 4-POBN/hydroxypentyl radical adducts. HPLC–EPR analyses showed that P_a and P_c are identical with P_1 and P_2, respectively. The results also indicated that P_1 and P_2 are two diastereoisomers of 4-POBN/1-methyl-4-hydroxybutyl radical adducts. Radical rearrangements of carbon-centered radicals were discussed for 1,4-hydrogen shifts, 1,5-hydrogen shifts and 1,6-hydrogen shifts, respectively (*22*, *23*). 1,5-Hydrogen shifts preferentially occur. 1,6-Hydrogen shifts and longer shifts have also been found. The possibility of 1,3-hydrogen shifts has been much investigated, but it is not certain if any actually occur. 1,4-Hydrogen shifts are definitely known, but are still not very common. 1-Hydroxypentyl radical possibly forms in the reaction mixture of 1-pentanol with Fenton reaction system because elimination of α proton in pentanol readily occurs (*24*, *25*). The 1-hydroxypentyl radical is convertible into 5-hydroxypentyl radical through 1,5-hydrogen shifts. 1-Methyl-4-hydroxybutyl radical also possibly forms from 1-hydroxypentyl radical through 1,4-hydrogen shifts. Thus, the five peaks (P_a, P_b, P_c, P_d and P_e) on the HPLC–EPR elution profile of the reaction mixture of 1-pentanol with Fenton reaction system are tentatively assigned as follows: P_a and P_c, two diastereoisomers of 4-POBN/1-methyl-4-hydroxybutyl radical adducts; P_b, 4-POBN/5-hydroxypentyl radical adduct; P_d and P_e, two diastereoisomers of 4-POBN/1-hydroxypentyl radical adduct.

We focused on the effects of Mb on the radical generation in mixed-function oxidases of the endoplasmic reticulum in this article. Mb stimulated the radical formation form lipid peroxides (Fig. 6). On the other hand, iron ions participate in both steps, the LOOH-generation step and radical-formation step from the LOOH in the control reaction. Iron ions rather than Mb seem to play a significant role in the formation of the free radicals. However, since iron ions may be supplied from Mb (*26*), Mb could be relevant to acute renal failure in rhabdomyolysis *in vivo*.

CONFLICT OF INTEREST

None declared.

REFERENCES

1. Finsterer, J., Zuntner, G., Fuchs, M., and Weinberger, A. (2007) Severe rhabdomyolysis after excessive bodybuilding. *J. Sports Med. Phys. Fitness* **47**, 502–505
2. Shah, S.V. and Walker, P.D. (1988) Evidence suggesting a role for hydroxyl radical in glycerol-induced acute renal failure. *Am. J. Physiol.* **255** (Renal Fluid Electrolyte Physiol. **24**), F438–F443
3. Zager, R.A., Burkhart, K.M., Conrad, D.S., and Gmur, D.J. (1995) Iron, heme oxygenase and glutathione: effects on myohemoglobinuric proximal tubular injury. *Kidney Int.* **48**, 1624–1634
4. Minigh, J.L. and Valentovic, M.A. (2003) Characterization of myoglobin toxicity in renal cortical slices from Fischer 344 rats. *Toxicology* **184**, 113–123
5. Salahudeen, A.K., Wang, C., Bigler, S.A., Dai, Z., and Tachikawa, H. (1996) Synergistic renal protection by combining alkaline-diuresis with lipid peroxidation inhibitors in rhabdomyolysis: possible interaction between oxidant and non-oxidant mechanisms. *Nephrol. Dial. Transplant.* **11**, 635–642
6. Holt, S., Reeder, B., Wilson, M., Harvey, S., Morrow, J.D., Roberts II, L.J., and Moore, K. (1999) Increased lipid peroxidation in patients with rhabdomyolysis. *Lancent* **353**, 1241
7. Zager, R.A. and Burkhart, K. (1997) Myoglobin toxicity in proximal human kidney cells: roles of Fe, Ca^{2+}, H_2O_2, and terminal mitochondrial electron transport. *Kidney Int.* **51**, 728–738
8. Holt, S. and Moore, K. (2000) Pathogenesis of renal failure in rhabdomyolysis: the role of myoglobin. *Exp. Nephrology* **8**, 72–76
9. Paller, M.S. (1988) Hemoglobin and myoglobin induced acute renal failure in rats: role of iron in nephrotoxicity. *Am. J. Physiol.* **255** (Renal Fluid Electrolyte Physiol. **24**), F539–F544
10. Paller, M.S. (1994) The cell biology of reperfusion injury in the kidney. *J. Investg. Med.* **42**, 632–639
11. Nath, K.A. and Norby, S.M. (2000) Reactive oxygen species and acute renal failure. *Am. J. Med.* **109**, 655–678
12. Baliga, R., Zhang, Z., Baliga, M., and Shah, S.V. (1996) Evidence for cytochrome P-450 as a source of catalytic iron in myoglobinuric acute renal failure. *Kidney Int.* **49**, 362–369
13. Iwahashi, H. (2008) High performance liquid chromatography/electron spin resonance/mass spectrometry analyses of lipid-derived radicals in 6 in *Method in Molecular Biology. Advanced protocols in Oxidative Stress* (Armstrong, D., ed.) Vol. 477, pp. 65–73, Humana Press, New York
14. Gever, G. and Hayes, K. (1949) Alkylhydrazines. *J. Org. Chem.* **14**, 813–818
15. Iwahashi, H. (2000) Some polyphenols inhibit the formation of pentyl radical and octanoic acid radical in the reaction mixture of linoleic acid hydroperoxide with ferrous ions. *Biochem. J.* **346**, 265–273
16. Iwahashi, H., Albro, P.W., McGown, S.R., Tomer, K.B., and Mason, R.P. (1991) Isolation and identification of α-(4-pyridyl-1-oxide)-*N-tert*-butylnitrone radical adducts formed by the decomposition of the hydroperoxides of linoliec acid, linolenic acid, and arachidonic acid by soybean lipoxygenase. *Arch. Biochem. Biophys.* **285**, 172–180
17. Rota, C., Barr, D.P., Martin, M.V., Guengerich, F.P., Tomasi, A., and Mason, R.P. (1997) Detection of free radicals produced from the reaction of cytochrome P-450 with linoleic acid hydroperoxide. *Biochem. J.* **328**, 565–571
18. Cadenas, E. and Sies, H. (1982) Low level chemiluminescence of liver microsomal fractions initiated by tert-butyl hydroperoxide. *Eur. J. Biochem.* **124**, 349–356
19. Carter, W.P.L., Darnall, K.R., Lloyd, A.C., Winer, A.M., and Pitts Jr., J.N. (1976) Evidence for alkoxy radical isomerization in photooxidations of C_4-C_6 alkanes under simulated atmospheric conditions. *Chem. Phys. Lett.* **42**, 22–27
20. Niki, H., Maker, P.D., Savage, C.M., and Breitenbach, L.P. (1981) An FT IR study of the isomerization and O_2 reaction of n-butoxy radicals. *J. Phys. Chem.* **85**, 2698–2700
21. Lazar, M., Rychly, J., Klimo, V., and Pelikan, P. (1989) 3. Elementary reactions of free radicals in *Free Radicals in Chemistry and Biology*, pp. 43–128, CRC Press, Florida
22. Freidlina, R.K. and Terent'ev, A.B. (1977) Free-radical rearrangements in telomerization. *Acc. Chem. Res.* **10**, 9–15
23. March, J. (1992) Rearrangements in *Advanced Organic Chemistry*. Fourth edn, pp. 1051–1157, John Wiley & Sons, New York
24. Kotake, Y., Kuwata, K., and Janzen, E.G. (1979) Electron spin resonance spetra of diastereomeric nitroxyls produced by spin trapping hydroxyalkyl radicals. *J. Phys. Chem.* **83**, 3024–3029
25. Iwahashi, H., Parker, C.E., Mason, R.P., and Tomer, K.B. (1990) Radical identification by liquid chromatography/thermospray mass spectrometry. *Rapid Commun. Mass Spectrom.* **4**, 352–354
26. Hill-Kapturczak, N., Chang, S., and Agarwal, A. (2002) Heme oxygenase and the kidney. *DNA Cell Biol.* **21**, 307–321